Temperature compensated, humidity insensitive, high-Tg TOPAS FBGs for accelerometers and microphones

Stefani, Alessio ; Yuan, W.; Markos, C.; Rasmussen, Henrik K.; Andresen, S.; Guastavino, R.; Nielsen, F. K.; Rose, B.; Jespersen, O.; Herholdt-Rasmussen, N.; Bang, Ole

Published in:
Proceedings of SPIE, the International Society for Optical Engineering

Link to article, DOI:
10.1117/12.977859

Publication date:
2012

Document Version
Peer reviewed version

Temperature compensated, humidity insensitive, high-T_g TOPAS FBGs for accelerometers and microphones

A. Stefani[a], W. Yuan[b], C. Markos[c], H.K. Rasmussen[d], S. Andresen[e], R. Guastavino[e], F.K. Nielsen[e], B. Rose[f], O. Jespersen[f], N. Herholdt-Rasmussen[f], O. Bang*[a]

[a] DTU Fotonik, Dept. of Photonics Engineering, Technical University of Denmark, 2800 Kgs. Lyngby, Denmark
[b] Singapore Institute of Manufacturing Technology, 71 Nanyang Drive, 638075, Singapore
[c] Dept. of Computer Engineering and Informatics, University of Patras, 26500, Patra, Greece
[d] Dept. of Mechanical Engineering, Technical University of Denmark, 2800 Kgs. Lyngby, Denmark
[e] Brüel & Kjær Sound & Vibration Measurement A/S, Skodsborgvej 307, 2850 Nærum, Denmark
[f] Ibsen Photonics A/S, Ryttermarken 15-21, 3520 Farum, Denmark
*oban@fotonik.dtu.dk

ABSTRACT

In this paper we present our latest work on Fiber Bragg Gratings (FBGs) in microstructured polymer optical fibers (mPOFs) and their application as strain sensing transducers in devices, such as accelerometers and microphones. We demonstrate how the cross-sensitivity of the FBG to temperature is eliminated by using dual-FBG technology and how mPOFs fabricated from different grades of TOPAS with glass transition temperatures around 135°C potentially allow high-temperature humidity insensitive operation. The results bring the mPOF FBG closer to being a viable technology for commercial applications requiring high sensitivity due to the low Young's Modulus of polymer.

Keywords: FBG, mPOF, high-T_g, sensors, accelerometer, microphone.

1. INTRODUCTION

Most optical fibers are constructed from silica (glass). In 1979 it was discovered that the cores of such fibers displayed photosensitivity to UV light. This phenomenon remained a curiosity for about a decade until it was realised that a spatially periodic modification to the refractive index along the core of the fiber could be induced by exposing a short section of the fiber to a spatially varying intensity pattern of UV light, usually produced by interfering two beams of coherent UV light incident on the side of the fiber. Such a device is known as a FBG and it has the property of reflecting light of essentially one wavelength, while allowing all other wavelengths to pass. The precise reflected wavelength is initially set by the period of the inscribing UV light pattern, but once the grating is recorded the reflected wavelength is also influenced by the strain to which that region of fiber is subjected and this process offers the possibility of monitoring strain entirely optically.

Since the early nineties, reports on work on silica FBGs have outnumbered other optical fiber sensing technologies at the regular series of International Conferences on Optical Fiber Sensors. The basic aspects of the technology are now quite mature and the technology has been commercialised for more than 10 years. Silica optical fiber strain gauges offer the following advantages over conventional electrical strain and vibration transducers.

- Immunity to electromagnetic interference
- Possibility for multiplexing several sensors at different wavelengths on a single fiber
- Light weight and small size
- Low optical loss
- Remote sensor deployment, several km from the read-out system
- Operation at high temperature (>500 °C) possible

In many ways silica is a very good material from which to construct strain sensors. However, the silica optical fiber does have some significant limitations:

- Silica is a stiff material (Young's modulus = 73 GPa) and so when silica fiber sensors are used to monitor compliant or elastic structures, the silica fiber can act to reinforce the structure, so that the local strain experienced by the fiber is much smaller than the true background strain.
- The fracture strain of silica (especially under repeated strain cycling) is much less than some structures of interest (e.g. some composite materials), limiting its range of applicability.

Both these deficiencies can be overcome through the use of polymer optical fibers (POFs), which offer some additional potential advantages:

- There is a huge range of polymeric materials that could be used to create POFs providing different physical and chemical properties, such as PMMA, TOPAS, and ZEONEX. The standard polymer PMMA has, e.g., a Young's modulus about 30 times lower than silica and a failure strain about 10 times higher
- The tools of organic chemistry may be used to modify POFs, either by adding functional groups directly to the polymer or doping the fiber with organic compounds. This offers access to a wide range of possibilities for realising specific chemical sensitivity, enhancing nonlinear effects or providing optical amplification.
- POFs are attractive for medical applications, particularly in-vivo, where the dangers associated with a potentially broken silica fiber are significant

For a review of FBG sensors we refer to the recent book [1], which also includes a chapter providing the state-of-the-art of polymer FBGs [2].

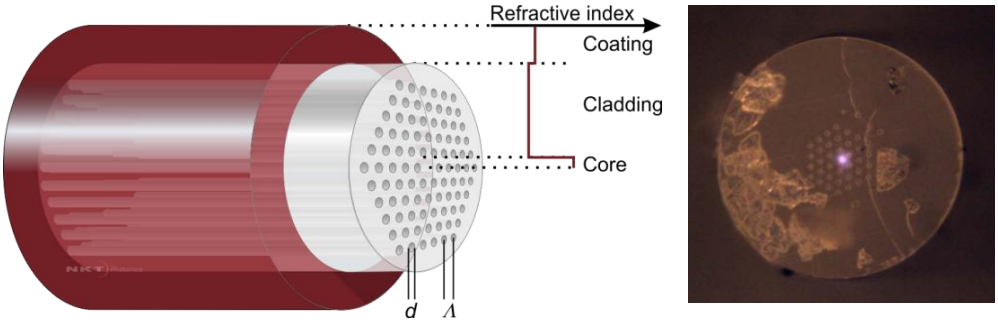

Figure 1. Left: mPOF hole structure with pitch Λ and hole diameter d, providing a lower average refractive index in the cladding than in the solid core. Right: Visible light being guided in a 3-ring mPOF fabricated at DTU.

We here focus on POF FBGs and in particular solid-core index-guiding microstructured POFs (mPOFs - see Fig. 1), because they can easily be made endlessly single-moded by designing the cladding hole structure to have a hole diameter d and distance between holes, or pitch Λ, so that the relative hole size d/Λ is less than 0.44. For an overview of mPOF technology we refer to the book [3]. Even though the first POF FBG and mPOF FBG was presented in 1999 [4] and 2005 [5], respectively, the polymer FBG sensing platform has not yet translated into a commercial sensor product, despite the obvious possibilities of improving the sensitivity and increasing the failure strain by using polymer instead of silica. The reason is the high loss of the single-mode POF/mPOF at the telecom wavelength 1550 nm, which means that 850 nm is a more appropriate wavelength of operation because of a much reduced loss and the availability of CMOS technology. The loss of an mPOF depends on the draw tension, the surface roughness of the holes, the outer fiber diameter, the fiber core size, and whether or not the fiber has been sealed after fabrication to avoid contamination of the holes [6]. Low loss requires a high draw tension, a large outer fiber diameter, and a large core diameter [6]. Thick highly multi-moded PMMA mPOFs with loss as low as 0.16 dB/m at 650 nm have been reported [6], but these are unsuitable for FBG sensing purposes. Single-mode 125 μm in diameter mPOF have a reported lowest loss around 1.6 dB/m [6]. Equally important for the slow progress in polymer FBG sensing is the fact that good cleaving and splicing equipment are not readily available commercially. In regards to the material properties of polymer, the strong dependence of the standard PMMA on humidity and the relatively low glass transition temperature of PMMA are also important factors, together with the inherent temperature sensitivity of FBG sensors of any fiber material.

Within the last 2 years several of the problems with the POF FBG sensor technology have been addressed: 850nm FBGs have been demonstrated in mPOFs and POFs [7-10]. FBGs have been written in mPOFs made of the novel polymer

TOPAS [11] and demonstrated to have a humidity sensitivity so weak that it cannot be detected in the humidity chamber [9]. Annealing the FBG has been shown to offer more stable short-term performance at both higher temperature and larger strain and to extend the operational temperature and strain range without hysteresis [12]. Tunable FBG writing over 12 nm has been demonstrated by stretching the fiber during writing and this has been used to demonstrate dual-FBG temperature compensation in single-mode PMMA mPOFs [10]. In terms of fiber handling, high-quality cleaving of TOPAS mPOFs has been demonstrated at 40°C, compared to 77.5°C for PMMA [13], which reflects the low glass transition temperature T_g = 85°C of the grade 8007 of TOPAS used so far [9,11,13]. Equally important, stable gluing of POFs and mPOFs to silica fibers have now been demonstrated [14,15].

These recent improvements have increased the confidence in the polymer FBG technology and allowed the first fabrication of a fiber-optical accelerometer based on both silica and polymer FBGs [14] and a clear demonstration of the improved sensitivity made available by the low Young's modulus of the POF [14]. Here we review some of the recent improvements and present the first fiber-optical microphone based on FBG technology. We go one step further and present the first FBG written in grade 5013 TOPAS with a glass transition temperature as high as T_g = 135°C, which could potentially provide operation temperatures up to 110°C, in addition to being humidity insensitive. Combined with dual-FBG temperature compensation, the high-T_g TOPAS FBGs can also be made temperature insensitive.

2. WRITING OF 850NM AND 1550NM FBGS IN MPOFS

All our FBGs have been written into mPOFs with the UV phase-mask technique using a 30 mW 325 nm CW HeCd laser (IK5751I-G, Kimmon) for illumination. The pattern imprinted into the fiber was determined by the phase mask (Ibsen Photonics), placed just above the fiber, whose period of 572.4 nm (1024.7 nm) was optimized for polymer fibers to give 850 nm (1550 nm) gratings. The outer fiber diameter was in all case about 125 μm, unless stated otherwise.

3. TOPAS FBG: HUMIDITY INSENSITIVITY AND HIGH TEMPERATURE WORKING RANGE

Research to date on POF gratings has essentially involved PMMA, which has an affinity for water and a moisture absorption uptake of 0.3% [16]. When PMMA FBGs are applied to temperature and strain sensing, the cross-sensitivity to humidity is thus a serious issue [17]. In contrast, TOPAS has a very low moisture absorption uptake of <0.01% [16], which makes it a very appealing alternative to address the humidity sensitivity problem suffered by PMMA.

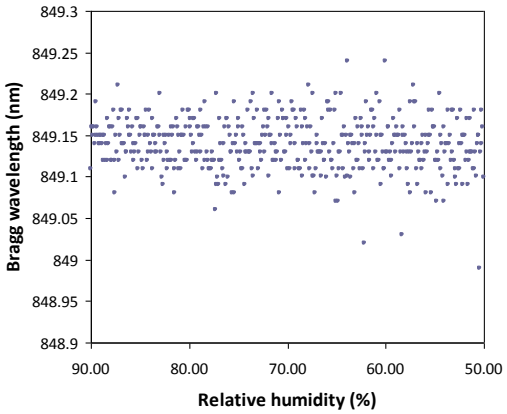

Figure 2. Humidity response of an 849 nm TOPAS mPOF FBG measured at Aston University [9]. The humidity was continuously decreased from 90% to 50% over a 4 hour time period (Figure adopted from [9]).

The humidity response of an 849 nm TOPAS mPOF FBG was examined in a humidity chamber (Sanyo Gallenkamp) at Aston University for 4 hours at 25 °C, where it was subject to a humidity gradually decreasing from 90% to 50%. The results are shown in Fig. 2 (adopted from [9]). Linear regression provides a slope of 0.26±0.12 pm/%, which gives a total shift of only about -10 pm over 40% [9]. Here the specified temperature stability of 0.3°C of the humidity chamber and the measured temperature sensitivity of the TOPAS mPOF FBG of -78pm/°C [9], must be considered. It means that a 0.3

ºC temperature rise would cause a wavelength shift of -23.4 pm. Consequently, the observed wavelength shift could be due to temperature drifts in the chamber alone. An upper limit on the magnitude of the humidity sensitivity can be calculated by considering a worst-case scenario, where we assume that there has been a temperature drop of 0.3 ºC over the 4 hour experiment, leading to a temperature induced positive wavelength shift of 23.4 pm. The observed net negative wavelength shift of -10pm would therefore require a contribution to the wavelength shift from humidity of -33.4 pm over the experiment or 0.83 pm/% relative humidity. Note that in [9] an upper limit of 0.7 pm/% was found by mistake by using a wrong FBG temperature sensitivity of -60 pm/ ºC. We stress that this is a worst case calculation and the actual sensitivity is likely to be much lower. In comparison a 1565 nm PMMA FBG displayed a sensitivity of 38.4±0.4 pm/% [17], which is over 46 times more than the maximum possible humidity sensitivity of the TOPAS FBG.

Humidity insensitivity is not the only interesting feature of TOPAS. In contrast to PMMA it is chemically inert, which provides interesting features for biosensing [18] and it has extremely low loss and low dispersion in the terahertz frequency regime [19]. More importantly for our purpose of strain sensing, TOPAS comes in different grades with different glass transition temperatures T_g, but still the same low water absorption. In particular, the TOPAS fibers used up to date are made of grade 8007 with T_g = 85ºC. In comparison PMMA has a glass transition temperature of about 115ºC [6] (can also change depending on the specific composition) and is thus considered a better material for real applications.

We have therefore fabricated the first mPOF in TOPAS grade 5013, which has T_g = 135ºC. The mPOF has 3 rings of holes in a triangular structure, just as the one depicted in Fig. 4. Loss measurements showed similar results to PMMA and previous TOPAS fibers. An 852 nm FBG was written into the fibers and taken to 110ºC in steps of about 10ºC, allowing 20 minutes at each step in order to reach the equilibrium. At each temperature step strain was applied up to over 2% and then released, in steps of about 0.5% strain. At each strain level 20 minutes were waited before measuring the spectrum. Figure 3(a) shows the grating spectrum at 105ºC when no strain was applied. Figure 3(b) shows the wavelength shift as function of strain at 105ºC for both increasing and decreasing strain. The response is quite linear and not different from the one at room temperature. This demonstrates the ability of this TOPAS FBG to perform at temperatures as high as 100ºC for more than 1 hour. In contrast our PMMA mPOF FBG "died" at 110ºC.

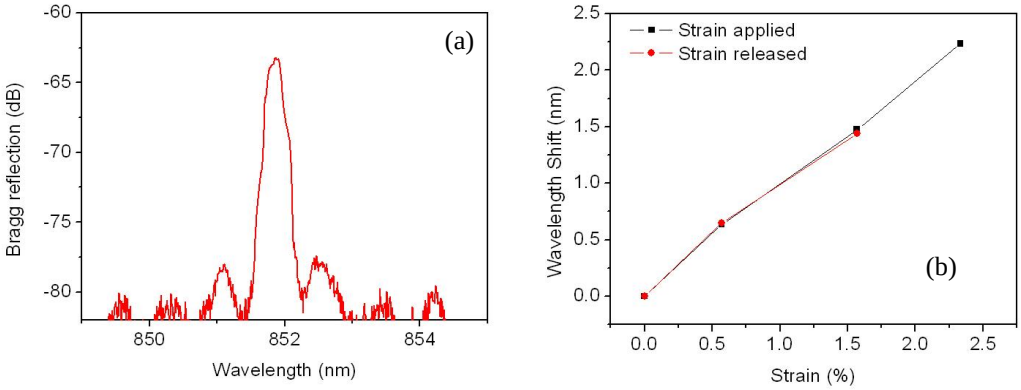

Figure 3. (a) Spectrum of the TOPAS mPOF FBG at 105°C and no strain applied. (b) Strain response of the TOPAS mPOF FBG at 105°C. 20 minutes were allowed to reach the equilibrium every time.

4. TEMPERATURE COMPENSATION

The cross-sensitivity of FBG strain sensors to temperature is inherent to both silica and polymer FBGs. A simple solution is to use a second closely spaced and strain free FBG with a different resonance wavelength to provide an independent control of the temperature. The difference in resonance wavelength between the two FBGs will then still measure the strain, but be independent of temperature, as was demonstrated for silica FBGs [20]. To fabricate two (or more) POF FBGs with closely spaced resonance wavelengths we have demonstrated a simple technique for highly controlled tuning of the resonance wavelength of a POF FBG written with the standard phase-mask technique using the *same phase-mask* [10]. By pre-straining the POF before writing the grating we can linearly tune the wavelength by 7 nm

using only 1% strain, as shown in Fig. 4. Going into the saturated regime we show 12 nm tuning with 2.25% strain using a force of only 0.5 N due to the low Young's modulus [10]. This tuning range is about 5 times higher than for silica fibers [21] and can prove useful for future multiplexed sensor applications of POFs. Let us briefly summarize the results of [10]:

A PMMA mPOF (see Fig. 4) was fabricated and strain was applied to it during UV-writing and measured with a v-groove axial force sensor (FSC102, Thorlabs). In the inset of Fig. 4 we show two FBGs with λ_B = 846.28 nm (FBG1) and 847.44 nm (FBG2) inscribed in the same fiber with 1 cm separation. After release both FBGs were unchanged after storage for more than 24 hours. We now use this dual-FBG as a strain sensor to demonstrate temperature compensated strain sensing. We control the temperature of both gratings and mechanically stretch FBG2, while FBG1 remains unstretched. The two ends of FBG2 are glued to micro-translation stages with a UV curable glue (OG116-31, Epotek), which is mechanically much stiffer than the PMMA mPOF, so that it does not influence the strain. One stage was kept fixed, while the other moved to apply axial strain to FBG2 manually with a low loading speed. The axial strain was determined by dividing the fiber longitudinal elongation by the length of fiber between the two gluing points. The longitudinal displacement accuracy of the translation stage is 1 µm. The strain-free FBG1 was taped onto the fixed stage. The FBGs were heated up with a resistive heater (TH60, Linkam) placed on top of them. A thermocouple was used to measure the temperature as close to the gratings as possible with an uncertainty around 0.3°C. A humidity sensor (C210, Lufft) was used to monitor the humidity near the two gratings with an uncertainty of 0.5 %rH.

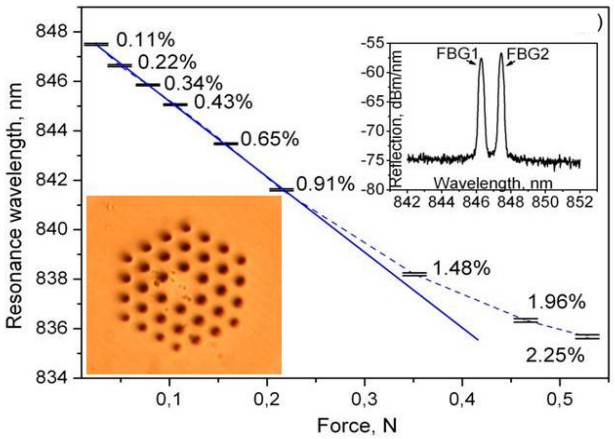

Figure 4. FBG resonance wavelength vs. force. The corresponding strain is given on the curve. Insets: PMMA mPOF used for grating writing and the reflection spectrum of a fabricated dual-FBG (adopted from [10]).

To emulate a practical situation and further confirm the temperature (humidity) compensation capability of our dual-FBG strain sensor, a strain-sensing experiment with a periodic temperature (humidity) change was carried out. As shown in Fig. 5, the strain applied to FBG2 was increased every 20 min., while the temperature (humidity) experienced by both gratings was cycled between 25°C (64%rH) and 35°C (48%rH) every 20 min. with a 10 min. offset from the strain increase.

In Fig. 5(a) we see how the strain recorded by FBG2 is strongly affected by the changing temperature (humidity), displaying the expected slow change in center wavelength of 770 pm with every 10°C change (given the -77pm/°C sensitivity of the FBG). The temperature dependence is effectively compensated by instead monitoring the difference in center wavelength between FBG2 and FBG1, as demonstrated in Fig. 5(b). In fact one cannot talk about a cross-sensitivity to temperature of this sensor, because the fluctuations observed in the zoom in Fig. 5(b) are so small that they are within the limits of the mechanical stability of the set-up. If we instead analyse the plateaus or periods with fixed strain, then the maximum standard deviation from the mean of 12 pm is found for the third plateau from 30 to 50 min. shown in the zoom. If we then divide the 12 pm with the change in average wavelength of 1687 pm going to the plateau 3 from plateau 2, then we get a measure for the maximum noise of 0.71%. This is obviously a low degree of noise given that the temperature is increased suddenly by 10°C during this 20 min. period, which shows the promise of the dual-FBG temperature compensation technique presented in [10].

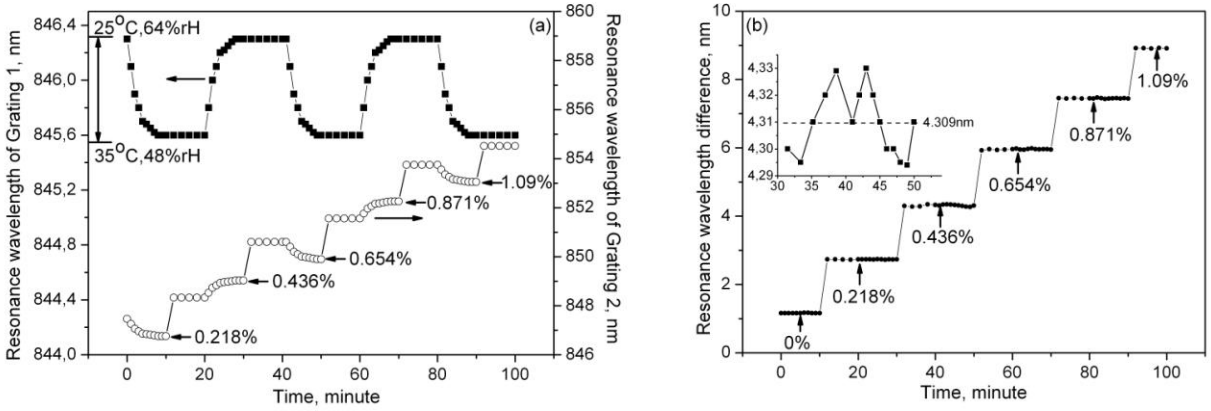

Figure 5. (a) Resonance wavelength of FBG1 and 2 for a temperature alternating between 25 and 35°C (humidity 64 and 38 %rH) every 20 min. while the strain applied to FBG2 alone was increased every 20 min. starting after 10 min. (b) Difference in resonance wavelength of FBG2 and 1. Inset: zoom from 31 to 50 min (adopted from [10]).

We note that in an earlier experiment, two broadband FBGs were inscribed in a large-core multi-mode mPOF at 1562 nm and 1545 nm using also a single phase-mask, by thermally annealing the first grating before writing the next [15]. Our method differs from the annealing technique, in that it is much more controllable and works with POFs regardless of their drawing conditions and whether they have been annealed or not. Furthermore, we are here able to apply it to narrow-band single-mode POFs to demonstrate closely packed FBGs ideal for future multiplexed POF FBG strain sensors. Most importantly, we have used the technique to present the first demonstration of temperature compensated FBG strain sensing in POFs.

5. ACCELEROMETER

Given the recent improvements in polymer FBG technology outlined above we have moved on to use it in practical sensing applications. A first example is a fiber-optical accelerometer, the basic construction of which is shown in Fig. 6. Initial results were presented at the Optical Fiber Sensor Conference in 2011 [22], but the fiber-optical accelerometer has now matured to a commercial product and here we report more in-depth studies. The acceleration is converted into strain by a mechanical transducer (Brüel & Kjær). The transducer has the shape of a fork and acceleration causes an increase in the separation between the arms of the fork. The FBG is attached to the fork and is therefore elongated to produce a wavelength shift proportional to the strain. The transducer is made so that the strain on the fiber is linearly dependent on acceleration, so that the Bragg wavelength shift corresponds to acceleration. The results presented in this section are a summary of our recently accepted paper [14] and the early results [22].

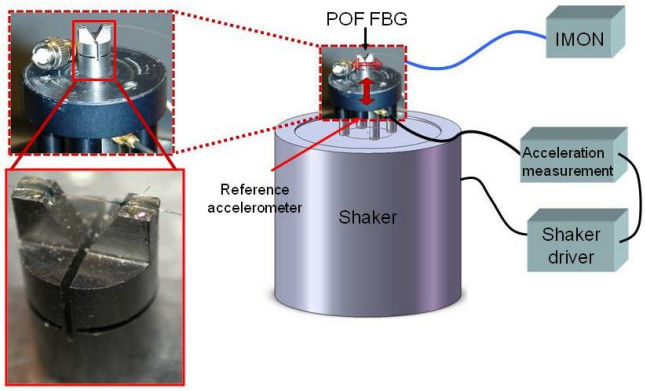

Figure 6. Schematic of the accelerometer characterization set-up with zooms of the inside of the FBG based accelerometer.

The test set-up is also shown in Fig. 6. A current driven shaker (Brüel & Kjær Type 4810) provides acceleration levels up to 15 g at frequencies up to 18 kHz. The FBG accelerometer is placed on top of the shaker platform. Underneath we placed a piezoelectric accelerometer with integrated charge preamplifier (Brüel & Kjær 4507) as a feedback reference for the current generator, in order to ensure that the shaker produced the desired acceleration level. The Bragg peak shift is measured with an I-MON 850-FW interrogator for 850 nm operation and an I-MON 80D-R interrogator for 1550 nm operation (both from Ibsen Photonics). The experiments were conducted at about 23°C in an air conditioned room to limit the Young's modulus temperature dependence. Several FBGs were written in PMMA mPOFs (same structure as in Fig. 4) with resonance wavelengths around 850 nm and 1550 nm (also different fiber thicknesses have been used) and FBGs in silica fibers with the same resonance wavelengths were used for comparison. Both the wavelength shift versus acceleration at a fixed frequency and the wavelength shift versus frequency at a fixed acceleration were characterized.

In order to test the sensitivity and operational range of the accelerometer, the response to a sine wave with a fixed frequency of 159.2 Hz was measured. The amplitude of the excitation is proportional to the acceleration and accelerations in the range from 0.1 g to 15 g (RMS) were used for the measurements shown in Fig. 7(a). We first investigate the influence of the fiber diameter on the sensitivity. To do so we compare in Fig. 7(a) the response of an accelerometer based on an 850 nm FBG in two PMMA mPOFs with an outer diameter (OD) of 160 µm (solid red line) and 130 µm (solid blue line), respectively. The sensitivity is, as expected, lowest for the accelerometer using a thick fiber, simply because a larger cross-sectional fiber area translates into a higher spring constant. Here the sensitivity drops from 5.9 pm/g to 4.22 pm/g with the 30 µm increase in OD. With the influence of the fiber diameter in mind we can now compare the sensitivities of corresponding polymer and silica FBG accelerometers. The black solid and dashed lines show the response of a 1550 nm FBG accelerometer using a 130 µm OD mPOF and an 80 µm OD silica fiber, respectively. Both show a linear response in the whole measurement range of 0.1-15 g, but the sensitivity of the mPOF accelerometer is about 3 times higher than the corresponding silica fiber accelerometer (15.2 pm/g against 5.1 pm/g), despite that the mPOF has a 50 nm larger diameter. The same improved sensitivity is found for the FBG accelerometer operating at 850 nm, where the 130 µm OD mPOF gives a sensitivity of 5.9 pm/g (solid blue line), which is 3.3 times the sensitivity of 1.8 pm/g obtained with a thinner 125 µm OD silica fiber (dashed blue line).

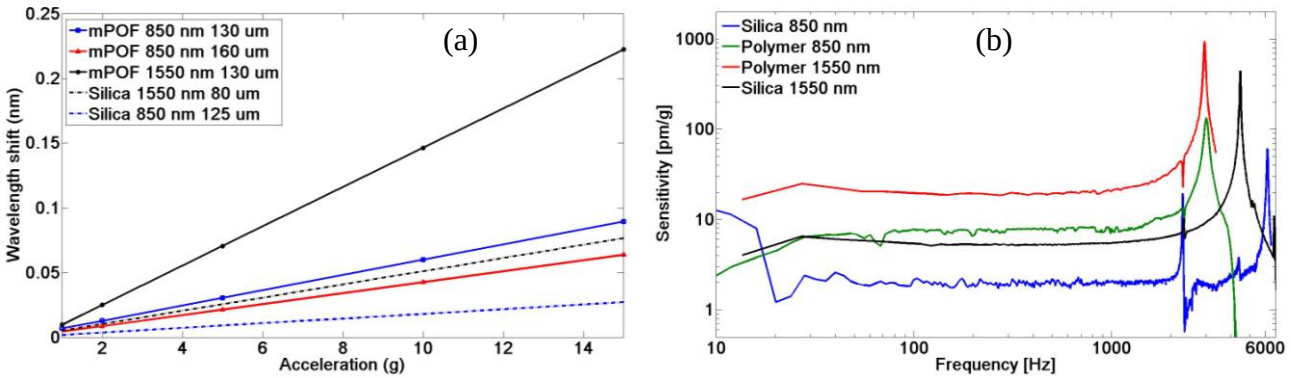

Figure 7. (a) Bragg wavelength shift vs. acceleration for accelerometers based on 1550nm silica FBGs (80 µm OD, dashed black) and 850nm silica FBGs (125 µm OD, dashed blue) and mPOF, FBGs with resonance wavelength of 1550 nm (130 µm OD, solid black) and 850 nm (solid blue line for 130 µm OD and solid red line for 160 µm OD). (b) Frequency response of the investigated accelerometers normalized to the applied acceleration of 1 g (adopted from [14]).

From Fig. 7(a) we also observe that the sensitivity decreases when the Bragg wavelength decreases, which is seen for both the mPOF and silica fiber based accelerometers. This is a well-known effect basically due to the fact that the same elongation is transduced to a wavelength shift proportional to the resonance wavelength. The acceleration in Fig. 7(a) is limited to 15 g because of the shaker limit. It is important to note that this corresponds to a wavelength shift of less than 300 pm and a strain of less than 0.02 %. Given that the linear response regime of polymer fibers is much higher it is evident that the mPOF FBG accelerometer can measure very high accelerations.

In Fig. 7(b) we show the frequency response for a fixed acceleration of 1 g for 1550 nm and 850 nm operated FBG accelerometers based on mPOF and silica FBGs. The response has been normalized to the applied acceleration. For all the FBGs, the accelerometer shows a flat response for frequencies up to about 1 kHz. When using silica FBGs the resonance frequency is higher because of the stiffness of the fiber. A more compliant fiber, such as the mPOF, lowers the system resonance frequency. The resonance frequency is close to 3 kHz for both mPOF based accelerometers, while it is 4.4 kHz when using the 80 µm 1550 nm silica FBG and 6.1 kHz for the 125 µm 850 nm silica FBG. The two mPOF FBG based accelerometers have the same resonance since they use the same fiber, while the silica FBGs are written in two different fibers. The thicker fiber shows a higher resonance because of the system being stiffer. The positive side is that a more compliant fiber has a higher sensitivity. In fact it is possible to see that the mPOF based accelerometers have a sensitivity about four times higher than the corresponding silica based ones. In order to take into account both factors a figure of merit is often used when characterizing accelerometers, which is the product of the sensitivity and the square of the resonance frequency. For accelerometers at both 1550 nm and 850 nm this figure of merit is bigger when using a polymer fiber [14].

It must be considered that for this particular figure of merit, an increase in thickness of the fiber would in fact give an advantage since the gain in resonance frequency counts more than the gain in sensitivity (for example in the 850 nm accelerometers the difference in figure of merit between polymer and silica is lower than for the 1550 nm ones because the fiber is thicker). In any case, the choice of the accelerometer is often given by the particular application for which it is intended. Disregarding the resonance frequency and looking only at frequencies lower than 1 kHz, the mPOF FBG based accelerometers have better performances than the silica ones for both 850 nm and 1550 nm operation.

6. MICROPHONE

With a similar working principle as that of the accelerometer, in which the acceleration was transduced by means of a mechanical fork into elongation of the Bragg grating, we have also fabricated the first FBG based optical microphone. In the case of the microphone the silica FBG simply has too low sensitivity to be relevant for human voice detection and thus we use only polymer FBGs. In the microphone housing a membrane is placed in contact with the mechanical fork, which transduces the sound pressure into elongation of the grating. Sound frequency and pressure amplitude can then be detected through wavelength shift. The realized microphone is shown in Figure 8. The interrogation system is the same as for the accelerometer and consists of an I-MON 850-FW (Ibsen Photonics). The FBG was written in a PMMA three ring mPOF (see Fig. 4) with a resonance wavelength around 850 nm, where the fast CMOS electronics allows detection of audio frequencies. The grating length is just above 4 mm.

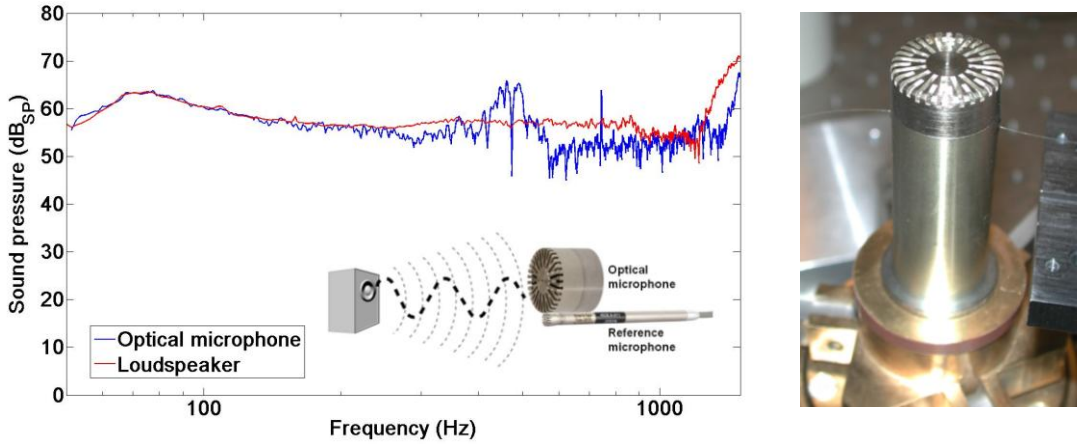

Figure 8. Left: frequency response of the fiber-optical microphone and of the test loudspeaker. Inset: sketch of the characterization set-up. Right: picture of the optical microphone.

The microphone was tested by using a loudspeaker as sound source and a reference microphone in order to determine the actual sound field at the optical microphone. A sketch of the measurement set-up is shown in the inset of Fig. 8. Figure 8 also shows the frequency response of the reference microphone and of the optical microphone (it has to be noted that the optical microphone response is wavelength shift and has been normalized in order to be compared with the reference). The frequency range used in the measurement is 50 Hz to 2 kHz. Although conventional microphones are made to work

up to 20 kHz, the limit for the human ear, frequencies from 300 Hz to 4 kHz cover the normal voice range (frequency range generally used in telephone microphones).

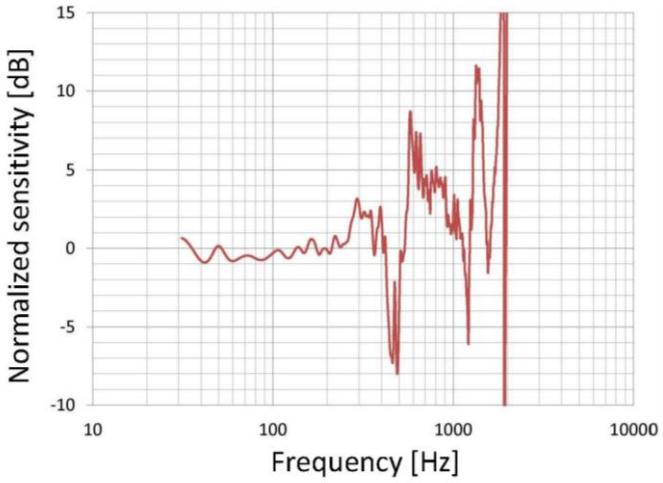

Figure 9. Microphone sensitivity relative to the sensitivity 0.01 nm/Pa at 250 Hz as a function of frequency.

The sensitivity of the microphone can be calculated by dividing the optical microphone response to that of the reference. The results shown in Fig.9 show a quite flat sensitivity up to 300 Hz and a strong resonance at around 500 Hz. The sensitivity itself would be enough for detection of sound with not too high loudness (normal speech level), because the narrowband noise level is quite low (0.003 pm wavelength shift). However, when looking at the time trace instead of the frequency trace, the noise is integrated on the whole bandwidth, thereby decreasing drastically the signal to noise ratio.

7. CONCLUSIONS

In conclusion we have demonstrated significant progress towards establishing a polymer FBG technology platform based on the polymer TOPAS, which potentially allows operation temperatures up to 110^{o}C of highly sensitive polymer FBGs that are humidity insensitive and can have no cross-sensitivity to temperature by using dual-FBG technology. Given the demonstration of high-quality cleaving of the TOPAS fibers and stable gluing of them to silica fibers these results promise to overcome many of the limiting factors that have so far hindered polymer FBG strain sensors from successfully entering the FBG sensor market. First demonstrations of polymer FBG-based optical accelerometers and microphones have been presented.

ACKNOWLEDGMENTS

We would like to acknowledge support from the Danish National Advanced Technology Foundation.

REFERENCES

[1] Cusano, A., Cutolo, A., and Albert, J. (Eds.), [Fiber Bragg Gratings Sensors: Thirty Years from Research to Market], Bentham eBooks (April 2011).
[2] Webb, D.J. and Kalli, K., “Polymer fiber Bragg gratings”, in Cusano, A., Cutolo, A., and Albert, J. (Eds.), [Fiber Bragg Gratings Sensors: Thirty Years from Research to Market], Bentham eBooks (April 2011).
[3] Large, M.C.J., Poladian, L., Barton, G.W. and van Eijkelenborg, M.A., [Microstructured Polymer Optical Fibres], Springer, New York (2008).
[4] Xiong, Z., Peng, G.D., Wu, B. and Chu, P.L., “Highly tunable Bragg gratings in single-mode polymer optical fibers”, IEEE Photon. Technol. Lett. 11(3), 352-354 (1999).

[5] Dobb, H., Webb, D.J., Kalli, K., Argyros, A., Large, M.C.J. and van Eijkelenborg, M.A., "Continuous wave ultraviolet light-induced fiber Bragg gratings in few- and single-mode microstructured polymer optical fibers", Opt. Lett. 30(24), 3296-3298 (2005).
[6] Argyros, A., Lwin, R., Leon-Saval, S.G., Poulin, J., Poladian, L. and Large, M.C.J., "Low loss and temperature stable microstructured polymer optical fibers", J. Lightwave Technol. 30(1), 192-197 (2012).
[7] Johnson, I.P., Kalli, K. and Webb, D.J., "827nm Bragg grating sensor in multimode microstructured polymer optical fiber," Electron. Lett. 46(17), 1217-1218 (2010).
[8] Stefani, A., Yuan, W., Markos, C. and Bang, O., "Narrow bandwidth 850nm Fiber Bragg gratings in few-mode polymer optical fibers", IEEE Photon. Technol. Lett. 23(10), 660-662 (2011).
[9] Yuan, W., Khan, L., Webb, D.J., Kalli, K., Rasmussen, H.K., Stefani, A. and Bang, O., "Humidity insensitive TOPAS polymer fiber Bragg grating sensor", Opt. Express 19(20), 19731-19739 (2011).
[10] Yuan, W., Stefani, A. and Bang, O., "Tunable polymer Fiber Bragg Grating (FBG) inscription: Fabrication of dual-FBG temperature compensated polymer optical fiber strain sensors", IEEE Photon. Technol. Lett. 24(5), 401-403 (2011).
[11] Johnson, I.P., Yuan, W., Stefani, A., Nielsen, K., Rasmussen, H.K., Khan, L., Webb, D.J., Kalli, K. and Bang, O., "Optical fiber Bragg grating recorded in TOPAS cyclic olefin copolymer", Electron. Lett. 47(4), 271-272 (2011).
[12] Yuan, W., Stefani, A., Bache, M., Jacobsen, T., Rose, B., Herholdt-Rasmussen, N., Nielsen, F.K., Andresen, S., Sørensen, O.B., Hansen, K.S. and Bang, O., "Improved thermal and strain performance of annealed polymer optical fiber Bragg gratings," Opt. Commun. 284(1), 176-182 (2010).
[13] Stefani, A., Nielsen, K., Rasmussen, H.K. and Bang, O., "Cleaving of TOPAS and PMMA microstructured polymer optical fibers: Core-shift and statistical quality optimization", Opt. Commun. 285, 1825-1833 (2012)
[14] Stefani, A., Yuan, W., Andresen, S., Herholdt-Rasmussen, N. and Bang, O., "High Sensitivity Polymer Optical Fiber Bragg Grating Based Accelerometer", IEEE Photon. Technol. Lett. (accepted Feb. 5, 2012).
[15] Johnson, I.P., Webb, D.J., Kalli, K., Large, M.C., Argyros, A., "Multiplexed FBG sensor recorded in multimode microstructured polymer optical fibre", in Kalli, K., Urbanczyk W. (eds), [Photonic Crystal Fibres; 14-16 April; Brussels - Photonics Europe], Proc. of SPIE 7714, 77140D (2010).
[16] Khanarian, G., "Optical properties of cyclic olefin copolymers," Opt. Eng. 40, 1024-1029 (2001).
[17] Zhang, C., Zhang, W., Webb, D.J., and Peng, G.D., "Optical fibre temperature and humidity sensor," Electron. Lett. 46(9), 643-644 (2010).
[18] Emiliyanov, G., Jensen, J.B., Bang, O., Bjarklev, A., Hoiby, P.E., Pedersen, L.H., Kjaer, E. and Lindvold,L., "Localized biosensing with Topas microstructured polymer optical fiber", Opt. Lett. 32(5), 460-462 (2007).
[19] Nielsen, K., Rasmussen, H.K., Adam, A.J.L., Planken, P.C.M., Bang, O. and Jepsen, P.U., "Bendable, low-loss Topas fibers for the terahertz frequency range", Opt. Express 17(10), 8592-8601 (2009).
[20] Haran, F.M., Rew, J.K. and Foote, P.D., "A strain-isolated fibre bragg grating sensor for temperature compensation of fibre Bragg grating strain sensors," Meas. Sci. Technol. 9(8), 1163-1166 (1998).
[21] Zhang, Q., Brown, D.A., Reinhart, L., Morse, T.F., Wang, J.Q. and Xiao, G., "Tuning Bragg wavelength by writing gratings on prestrained fibers", IEEE Photon. Technol. Lett. 6(7), 839-841 (1994).
[22] Andresen, S., Nielsen, F.K., Licht, T.R., Rasmussen, M.N. and Kirkelund, M., "Fibre Bragg grating vibration transducer based on novel mechanical sensing element for monitoring applications", Proc. of SPIE 7753, 77537M (2011).